Size and shape engineering of ZnO nanoparticles

Renata Marczak, Robin Klupp Taylor, Michael Voigt, Doris Segets, Wolfgang Peukert
Institute of Particle Technology, Friedrich-Alexander-University Erlangen-Nuremberg, Cauerstr. 4, 91058 Erlangen, Germany

Introduction

Zinc oxide is an attractive material for a broad range of electronic, optical, and piezoelectric applications due to its direct band gap and excellent thermal, chemical, and structural properties. For example, ZnO has been suggested for use in application such as light emitting diodes,[1] transparent electrodes,[2] solar cells,[3] sensors,[4] and many other devices.[5]

Different synthesis routes have been developed, including solid-vapor phase thermal sublimation,[6] spray pyrolysis,[7] RF plasma synthesis,[8] sonochemical or microwave-assisted synthesis[9] and hydrothermal processing.[10] However, wet-chemical synthesis of ZnO is an area of particular interest, since it provides a low-temperature, economical way to produce various ZnO nanostructures.[11, 12] Growth from solution typically starts with nucleation and is followed by growth of the nuclei by addition of dissolved species until the metal cation concentration reaches the solubility of the oxide. Then particle ageing proceeds in the mother liquors. Synthesis conditions such as temperature,[13] the overall concentration of the precursors,[14] water concentration,[15] ions present in solution[16], and solvent[17] have been shown to impact particle nucleation and growth. Therefore, the investigation of ZnO nanoparticles is of great interest due to the wide range of potential applications for this material. Despite this, a thorough understanding of the optical, electronic and structural properties of ZnO nanoparticles with respect to their synthesis is still lacking. We tackled this problem by synthesizing ZnO nanoparticles with nanocrystal and nanorod form. Dynamic light scattering (DLS), absorption and emission spectroscopies, thermogravimetric analysis (TGA), X-ray powder diffraction (XRD), Fourier infrared spectroscopy (FTIR) as well as transmission and scanning electron microscopies (HRTEM and SEM) were employed to characterize and compare the nanoparticles composition, their shape, size and crystallinity. By varying different parameters of the synthesis processes like precursors and their concentrations, solvent used, surfactant, temperature, and reaction time we were able to control the size and shape of the particles. In particular we noted the tendency of ZnO nanocrystals to self-assemble into dense structures which preserve the anisotropic crystal structure.

Experimental session

All chemicals were analytical grade reagents used without further purification. ZnO nanoparticles were prepared from zinc acetate dihydrate in alcoholic solution under basic conditions. To learn more about the growth mechanism, we have performed the experiments in different ways.

Quasi-spherical ZnO nanoparticles were obtained using a preparation procedure adapted from Spanhel, Anderson[11] and Meulenkamp[12]. A 2.19 g (0.01 mol) of zinc acetate dihydrate was dissolved in 100 mL of boiling ethanol at atmospheric pressure and cooled down to the synthesis temperature. A white powder of anhydrous zinc acetate precipitated close to room temperature.[12] A 0.34 g (0.014 mol) sample of lithium hydroxide was dissolved in 100 mL of boiling ethanol and cooled to the synthesis temperature. Then, the lithium hydroxide solution was added dropwise to the zinc acetate solution under vigorous stirring. The reaction mixture became transparent after addition of about 1/3 volume of the

lithium hydroxide solution. The ZnO colloid was stored at ≤ 10 °C to prevent rapid particle growth. Next, the ZnO suspension was washed by repeated flocculation of ZnO affected by addition of n-heptane. The supernatant was removed by centrifugation and decantation. For colloidal characterization the ZnO flocculates were redispersed in ethanol. In order to obtain the powder, the ZnO flocculates were dried under nitrogen for about 5 minutes.

ZnO nanorods were prepared according to a method described by Harnack.[18] Briefly, 29.5 g (0.13 mol) of zinc acetate dihydrate was dissolved in 125 mL of methanol at 65 °C. Then, a solution of 14.8 g (0.23 mol) of potassium hydroxide in 65 mL of methanol was added. The reaction mixture was stirred for several days at 65 °C. During this time, flocculation of the nanoparticles was observed. The length and the width of the resulting nanorods depended on the reaction time. The length of the nanorods increased considerably with longer reaction times, but the width of the nanorods grew only slightly. The ZnO floccs were washed with methanol. The supernatant was removed by decantation and the sample was dispersed in chloroform.

Particle size distribution, zeta potential and conductivity of ZnO nanoparticle suspensions were determined via dynamic light scattering (DLS) using a Malvern Nano ZS Instrument with a 633 nm “red” laser. For each sample ten measurements were performed and the average value per sample was calculated. The optical properties of the nanoparticles were determined from Uv-vis absorption spectra recorded using a Cary 100 Scan Spectrometer (Varian) with a 10mm path length cuvette. Structural analysis of the ZnO nanoparticles was performed using a D8 Advance (Bruker AXS) X-Ray diffractometer (XRD) using Cu-Kα radiation (0.154 nm). HRTEM images were obtained using a Philips CM 300 UltraTwin microscope with the particles deposited on a standard copper grid supported carbon film. The SEM images were obtained by using a Zeiss Gemini Ultra 55 SEM operating at an acceleration voltage of 20kV.

Results and discussion

Quasi-spherical ZnO particles were formed by precipitation in ethanolic solution. The zinc acetate and lithium hydroxide solutions in ethanol were mixed at different temperature under vigorous stirring. In order to follow the progress of the oxide formation, the suspensions of the nanoparticles were aged in their mother liquors and the crystal growth was monitored by the photospectroscopy and DLS.

The influence of nanocrystal size on the electronic structure of semiconducting material is represented by the band gap increasing with decreasing of the particle sizes, which is attributed to the so-called quantum confinement effect. ZnO shows this effect for particles smaller than 8 nm.[19] Hence, the measurement of absorption spectra provides a convenient way to investigate particle growth. Figure 1 shows the absorption spectra of the ZnO suspension recorded immediately after the preparation (about 3 minutes) and performed in 20 minutes intervals for about 14 hours. Just after mixing the zinc acetate with the lithium hydroxide the absorbance spectrum shows a well-defined exciton peak, which suggests a very fast nucleation. In addition, a marked red shift in the absorption edge was observed during the early formation stage, an indication of fast crystal growth. These absorption measurements could also provide a qualitative indication of the crystal size distribution. The sharp excitonic peak in the absorption spectra in the case of small nanocrystals (at shorter times) is indeed indicative of the narrow size distribution of the nanoparticles in the sample. For the larger particles, sharp excitionic features are not present in the absorption spectra (at longer times), but only a broad and featureless absorption edge. The latter is due to the fact that a number of exciton peaks appears at different energies corresponding to different sized nanocrystals which overlap with each other. Therefore, the nanocrystals are expected to have a broadened size distribution as

the ageing time increased. This was confirmed by the number-weighted size distributions recorded by using DLS at different times during the aging of the particles (Figure 2).

The influence of the ageing temperature on the particle growth was also examined (data not shown). It was found that the particle size continued to evolve, even when stored at lower temperatures. The ability to obtain various particle sizes is based on the phenomena that the growth of the particles is governed by ageing temperature and time but also by the presence of the reaction byproduct lithium acetate during the ageing process. The reaction could be almost completely stopped by removing this byproduct by reversible flocculation of the ZnO nanoparticles by addition of n-heptane[12] and redispersing in ethanol or drying under nitrogen for about 5 minutes to get white powder. To verify this restriction on crystal growth, DLS, Uv-vis (not shown) and HRTEM (Figure 3) measurements were carried out on redispersed crystals flocculated at different temperatures and times of ageing.

Herein, we present also that the shape of the ZnO particles was sensitive to the overall concentration of the precursors and the solvent used. As we showed above at a zinc acetate dihydrate concentration in ethanol of below 0.01 mol quasi-sperical particles were formed, whereas mainly nanorods were formed at 10 times higher concentrations. The ZnO nanorods were prepared from zinc acetate dihydrate in methanolic solution hydrolyzed by potassium hydroxide. This colloidal solution was refluxed at 65 °C for different length of time. The formation of ZnO nanorods is based on oriented attachment of preformed ZnO quasi-spherical nanoparticles. The growth from individual particles by crystallographically oriented and partially fused dimers and oligomers to almost perfect rods was monitored by SEM (Figure 4). During the early stage of growth (up to 1.5 h), aggregated quasi-spherical particles are recognized. Longer refluxing led to a coexistence of spherical and already formed short rod-like aggregates (Figure 4c and 4d). HRTEM studies of particles at intermediate growth stages revealed aggregated dimers (Figure 5) where it is seen that the lattice planes of the constituent particles are almost perfectly aligned. Moreover, the lattice planes go straight through the contact area, that is, the particles are epitaxially fused together, the neck between the particles still being visible. This oriented aggregation was observed along the ZnO *c* axis (0002). In the final formed nanorods (Figure 4e) the necks between particles have been filled up since the faces parallel to the *c* axis are seen to be smooth. A possible explanation is that this occurs by conventional mechanism of dissolution and growth of primary particles, which might also result in an overall growth of the rods, especially after a long reflux time. Thus, Ostwald ripening assists the growth process by oriented attachment in order to yield finally high-quality nanorods.

Structural analysis of both of the ZnO samples, i.e. the nanospheres and nanorods, was performed by using X-Ray diffraction. In the XRD pattern of the ZnO nanoparticles presented in Figure 6 no impurity peaks are observed. All the diffraction peaks are well assigned to standard hexagonal phase ZnO with a wurtzite structure reported in JCPDS card (No. 36-1451, a = 3.249 Å, c = 5.206 Å). The broadening of the XRD peaks observed for the ZnO spheres is due to the small particle size.

Conclusions

We have shown that by varying different parameters of the wet synthesis processes like precursors and their concentrations, solvent used, temperature, and reaction time we were able to control the size and shape of the ZnO nanoparticles. The presented growth mechanisms of the spheres and rods offer excellent tools to design advanced materials with anisotropic properties.

References

1. Colvin, V. L.; Schlamp, M. C.; Alivisatos, A. P. *Nature* **1994**, *370*, 354.
2. Duran, P.; Capel, F.; Tartaj, J.; Moure, C. *Adv. Mater.* **2002**, *14*, 137.
3. (a) O'Regan, B.; Gra¨tzel, M. *Nature* **1991**, *353*, 737. (b) Quintana, M.; Edvinsson, T.; Hagfeldt, A.; Boschloo, G. *J. Phys. Chem. C* **2007**, *111*, 1035. (c) Zeng, L.; Dai, S.; Xu, W.; Wang, K. *Plasma Science & Technology* **2006**, *8*, 172. (d) Redmond, G.; Fitzmaurice, D.; Grätzel, M. *Chem. Mater.,* **1994**, *6*, 686.
4. (a) Yang, M.; Wang, D.; Peng, L.; Zhao, Q.; Lin, Y.; Wei, X. *Sens. Actuators B* **2006**, *117*, 80. (b) Rout, C. S.; Raju, A. R.; Govindaraj, A; Rao, C. N. R. *Solid State Commun.* **2006**, 136.
5. (a) Johnson, J. C.; Yan, H.; Schaller, R. D.; Haber, L. H.; Saykally, R. J.; Yang, P. *J. Phys. Chem. B* **2001**, *105*, 11387. (b) Zhang, X. T.; Liu, Y. C.; Zhang, L. G.; Zhang, J. Y.; Lu, Y. M.; Shen, D. Z., Xu, W.; Zhong, G. Z.; Fan, X. W.; Kong, X. G. *J. Appl. Phys.* **2002**, *92*, 3293.
6. Wang, Z. L. *J. Phys. Condens. Matter* **2004**, *16*, R829.
7. (a) Park, S. B.; Kang, Y. C. *J. Aeroslo Sci.* **1997**, *28*, S473. (b) Okuyama, K.; Lenggoro, I. W. *Chem. Eng. Sci.* **2003**, *58*, 537.
8. Sato, T.; Tanigaki, T.; Suzuki, H.; Saito, Y.; Kido, O.; Kimura, Y.; Kaito, C.; Takeda, A.; Keneko, S. *J. Cryst. Growth* **2003**, *255*, 313.
9. (a) Hu, X. L.; Zhu, Y. J.; Wang, S. W. *Mater. Chem. Phys.* **2004**, *88*, 421. (b) Hong, R. Y.; Shen, Z. H.; Li, H. Z. *J. Process Eng.* **2005**, *5*, 693.
10. (a) Zhang, H.; Yang, D.; Ji, Y.; Ma, X. Y.; Xu, J.; Que, D. L. *J. Phys. Chem. B* **2004**, *108*, 3955., (b) Liu, B.; Zeng, H. C. *J. Am. Chem. Soc.* **2003**, *125*, 4430.
11. Spanhel, L; Anderson, M. A. *J. Am. Chem. Soc.* **1991**, *113*, 2826.
12. Meulenkamp, E. A. *J. Phys. Chem. B* **1998**, *102*, 5566.
13. Wong, E. M.; Bonevich, J. E.; Searson, P. C. *J. Phys. Chem. B* **1998**, *102*, 7770.
14. (a) Pacholski, C.; Kornowski, A.; Weller, H. *Angew. Chem. Int. Ed.* **2002**, *41*, 1188. (b) Verges, M. A. Mifsud., A.; Serna, C. J. *J. Chem. Soc. Faraday Trans.* **1990**, *86*, 959.
15. Hu, Z.; Escamilla Ramirez, D. J.; Heredia Cervera, B. E.; Oskam, G.; Searson, P. C. *J. Phys. Chem. B* **2005**, *109*, 11209.
16. (a) Hu, Z.; Oskam, G.; Penn, R. L.; Pesika, N.; Searson, P. C.; *J. Phys. Chem. B*. **2003**, *107*, 3124. (b) Hu, Z.; Herrera Santos, J. F.; Oskam, G.; Searson, P. C.; *J. Colloid. Interface Sci.* **2005**, *288*, 313.
17. Hu, Z.; Oskam, G.; Searson, P. C. *J. Colloid Interface Sci.* **2003**, *263*, 454.
18. Harnack,O.; Pacholski, C.; Weller, H.; Yasuda, A.; Jurina M.; Wessels, J. M. *Nano Letters* **2003**, *3*, 1097.
19. (a) Koch, U.; Fojtik, A.; Weller, H.; Henglein, A. *Chem. Phys. Lett.* **1985**, *122*, 507., (b) Wong, E. M.; Bonevich, J. E.; Searson, P. C. *J. Phys. Chem. B* **1998**, *102*, 7770., (c) Brus, L. E. *J. Phys. Chem. B* **1986**, *90*, 2555.

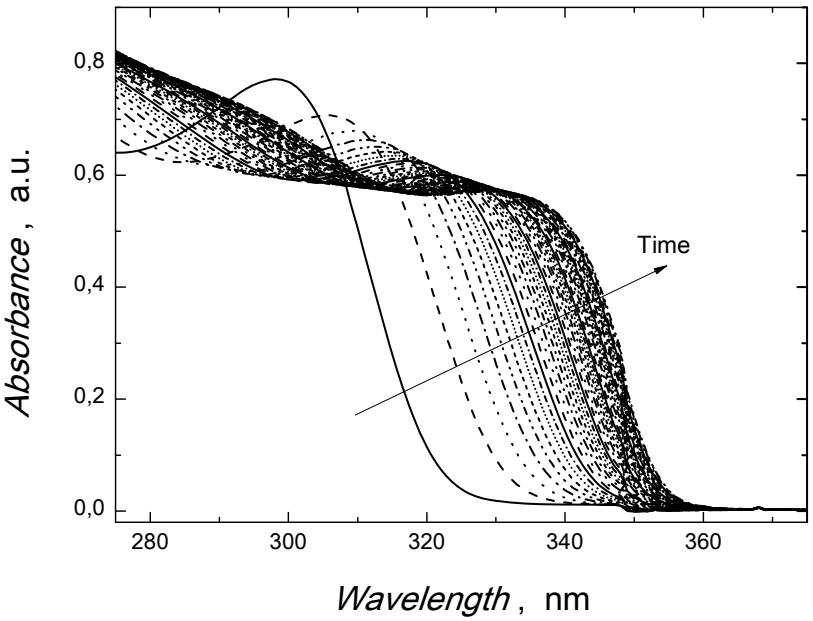

Figure 1. Room temperature absorption spectra recorded at different aging time of ZnO nanocrystals in ethanolic suspension. Red-shift in the absorption onset was observed between interval time 0 and 20 minutes.

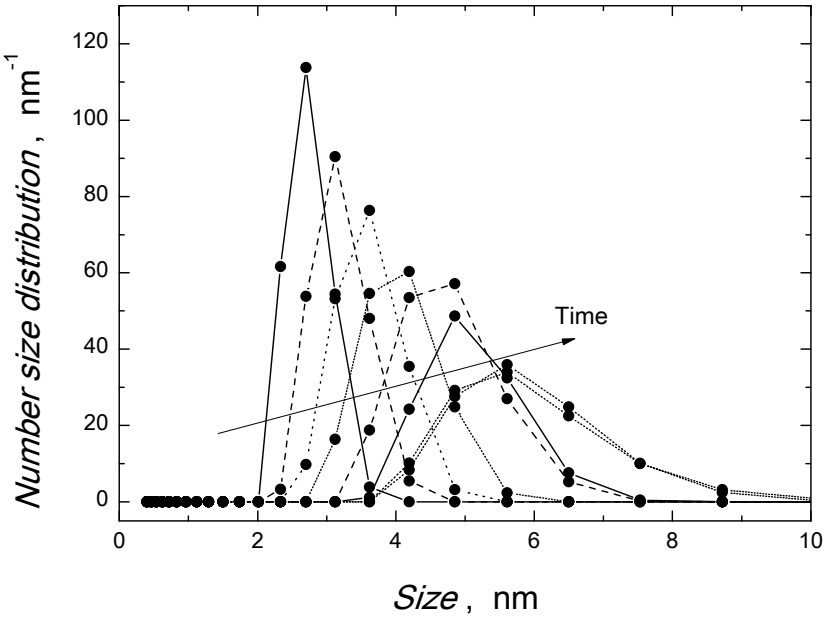

Figure 2. Number size distributions recorded by DLS at different aging time of the ZnO crystals in ethanolic suspension at 25 °C.

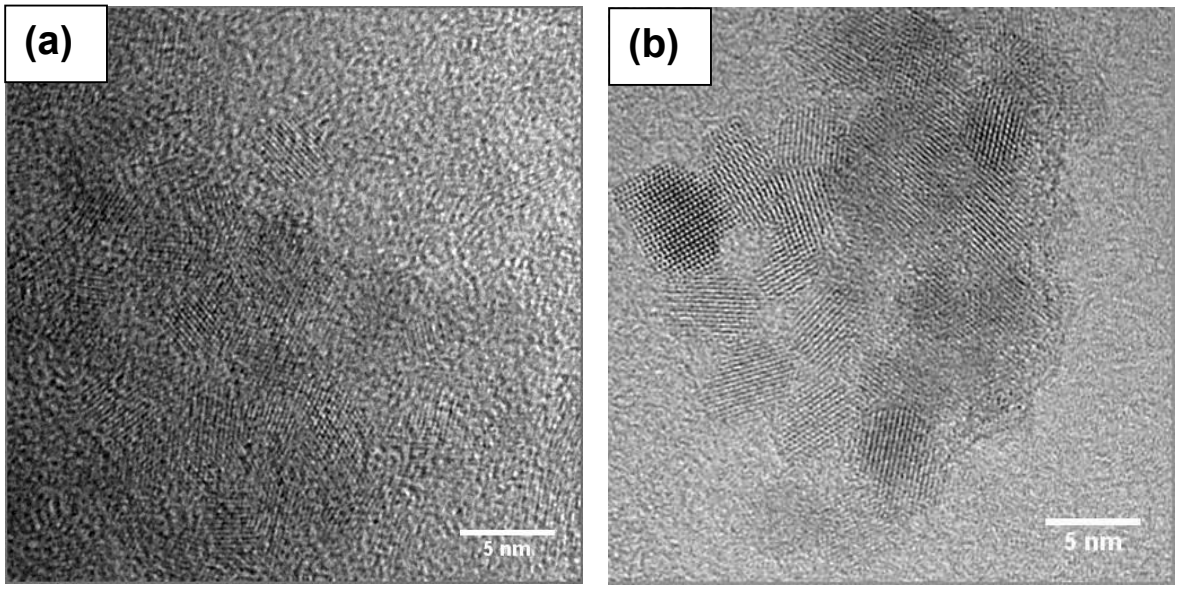

Figure 3. High resolution transmission electron microscopy images of ZnO nanospheres aged (a) for 4 h at 25 °C and (b) for 4 h at 35 °C. The crystalline nature of the ZnO nanoparticles is evidenced by the clearly observed lattice features.

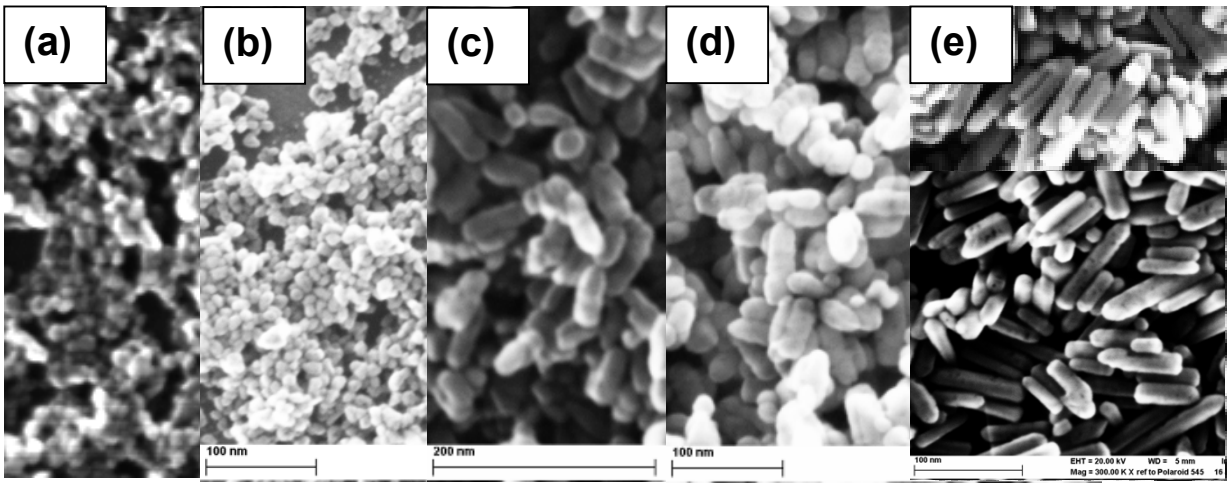

Figure 4. Scanning electron microscopy images of ZnO nanoparticles taken at different refluxing times: (a) 5, (b) 90, (c) 150, (d) 300 and (e) 1860 minutes.

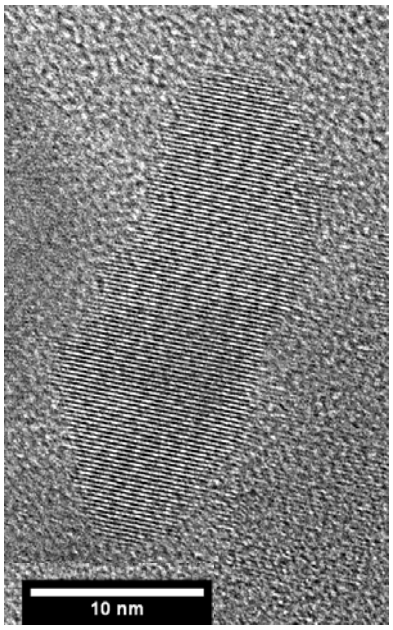

Figure 5. High resolution transmission electron microscopy image of the ZnO concentrated solution after reflux for 4 h showing dimers formation by oriented attachment. The crystalline nature of the ZnO nanoparticles is evidenced by the clearly observed lattice features.

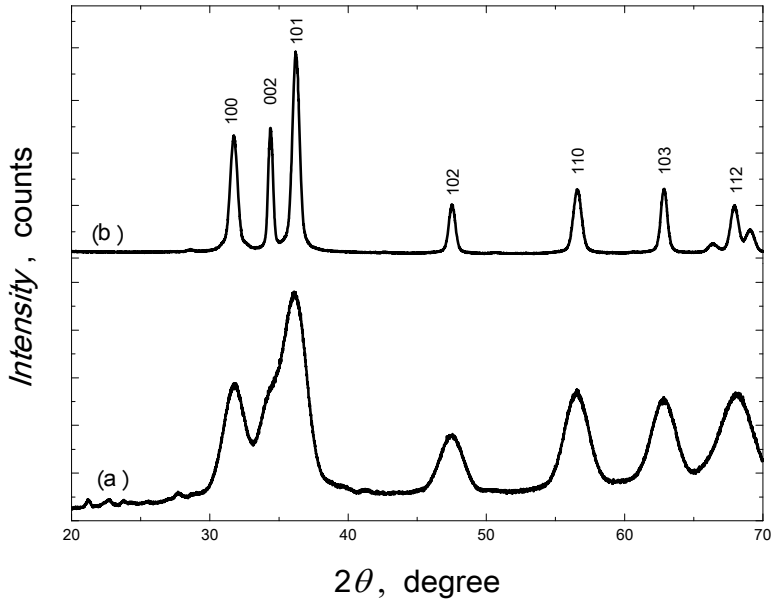

Figure 6. X-ray pattern of (a) ZnO nanospheres and (b) ZnO nanorods. All peaks correspond to ZnO wurtzite structure. The broadness of the XRD peaks reveals the nanocrystalline nature of the ZnO powders.